ELSEVIER

Journal of Nuclear Materials 290–293 (2001) 930–934

journal of nuclear materials

www.elsevier.nl/locate/jnucmat

The effect of divertor tile material on radiation profiles in LHD

B.J. Peterson [a,*], S. Masuzaki [a], R. Sakamoto [a], K. Sato [a], S. Inagaki [a], A. Sagara [a], S. Ohdachi [a], Y. Nakamura [a], N. Noda [a], Y. Xu [a], J.E. Rice [b], N. Ashikawa [c], S. Yamamoto [d], M. Takechi [d], K. Toi [a], S. Morita [a], M. Goto [a], K. Narihara [a], N. Inoue [a], Y. Takeiri [a], M. Sato [a], M. Osakabe [a], K. Tanaka [a], T. Tokuzawa [a], S. Sakakibara [a], M. Shoji [a], K. Kawahata [a], O. Kaneko [a], N. Ohyabu [a], H. Yamada [a], A. Komori [a], K. Yamazaki [a], S. Sudo [a], O. Motojima [a]

[a] *National Institute for Fusion Science, Toki-shi, Gifu-ken 509-5292, Japan*

[b] *Plasma Science and Fusion Center, Massachusetts Institute of Technology, Cambridge, MA 02139-4294, USA*

[c] *Graduate University for Advanced Studies, Hayama-machi, Kanagawa-ken 240-0193, Japan*

[d] *Department of Energy Engineering and Science, Nagoya University, Nagoya 464-01, Japan*

Abstract

In the large helical device (LHD) radiation profiles measured using arrays of resistive metal, foil bolometers are used to investigate the change in radiation resulting from a replacement of stainless steel divertor plates with graphite tiles between the second and third experimental campaigns. In particular, for the magnetic configuration of $R_{\text{axis}} = 3.6$ m and at line averaged densities below 3×10^{19} m^{-3}, a reduction of the radiated power fraction from 35% in the second campaign to down to 12% in third campaign was observed. Comparing similar shots (in terms of discharge parameters) from the second and third cycles the core ($0 < r/a < 0.79$) radiation fraction was reduced from 44% to 30% of the total radiation. Spectroscopic measurements show a corresponding decrease in radiation from iron. Comparing long pulse discharges the radiated power fraction reduced from greater than 67% during the density limiting oscillation observed in the second campaign to 20% during the third campaign with a reduction in the respective core radiation fractions from 63% to 37%.

Keywords: LHD; Impurity radiation; Divertor material

1. Introduction

One of the most serious consequences of plasma surface interactions is the introduction of impurities into the plasma and the resulting degradation of plasma performance due to radiative cooling and fueling gas dilution [1]. Therefore, plasma facing components and surface conditioning are chosen in order to reduce these effects and improve plasma performance. Additionally, various phenomena have been observed in fusion plasmas, which are related to radiation of impurities and which can detrimentally affect the plasma performance such as edge-localized modes [2] and MARFE [3].

In addition to spectroscopic measurements, spatially resolved radiated power measurements obtained from tomographic inversion of data from bolometric arrays can be a useful tool for diagnosing the role of impurity radiation on plasma performance. While the lighter impurities such as carbon and oxygen should radiate mainly from the edge of the plasma where the temperatures are low, heavier metallic impurities should radiate from the higher temperature core. Therefore, by using measured radiation profiles together with knowledge of the impurity makeup from spectroscopic data we can infer which impurities are contributing to the radiation

* Corresponding author. Tel.: +81-572 58 2239; fax: +81-572 58 2624.

E-mail address: peterson@LHD.nifs.ac.jp (B.J. Peterson).

0022-3115/01/$ - see front matter
PII: S 0 0 2 2 - 3 1 1 5 (0 0) 0 0 4 6 0 - 8

from various parts of the plasma. In this paper, we investigate the effects of divertor tile material in the large helical device (LHD) by comparing measured radiation profiles of shots having similar discharge parameters. To the greatest extent possible, when comparing two shots we have tried to find discharges where the only significant difference was the variable of interest in order to see the effect of the change of this variable. In addition, care has been taken to survey other discharges from the same experimental sequence to insure that the selected discharges are representative of that sequence.

2. LHD and diagnostics

LHD is a $l = 2$, 10-field period heliotron device with a nominal major radius of 3.9 m and an average minor radius of 0.6 m [4]. Data used in this study, were taken with the two most common magnetic configurations with a vacuum magnetic axis positions of $R_{\mathrm{axis}} = 3.6$ and 3.75 m, respectively. A maximum magnetic field of 2.9 T at the magnetic axis is produced using the main helical coil set and three sets of poloidal field coils, all of which are superconducting. The magnetic coil sets naturally produce an open double-null helical divertor. The divertor armor tiles were made of stainless steel (SS) plates during the first and second experimental campaigns and replaced with graphite for the third campaign. The vacuum vessel walls are stainless steel and were covered with SS armor for the third campaign. Plasmas are produced using ECH startup and maintained and heated with two tangential NBI beam lines having opposite orientations depositing 1–2 MW of power each to the plasma. Each beam line is fitted with a graphite beam dump to absorb the shine-through power. Wall conditioning used in LHD includes helium glow discharge cleaning, hydrogen glow discharge cleaning and titanium gettering. Helium glow discharge cleaning uses a bias voltage of 150 V and Hydrogen glow discharge cleaning uses a bias voltage of 200 V. Titanium gettering was carried out in the later half of the third campaign covering approximately 30% of the vacuum vessel surface.

Radiation profiles are measured using a 32-channel bolometer array in two cameras. Seventeen of these channels view the main plasma and are used in a tomographic inversion to get the radiation profile as a function of the minor radius [5]. Spectroscopic

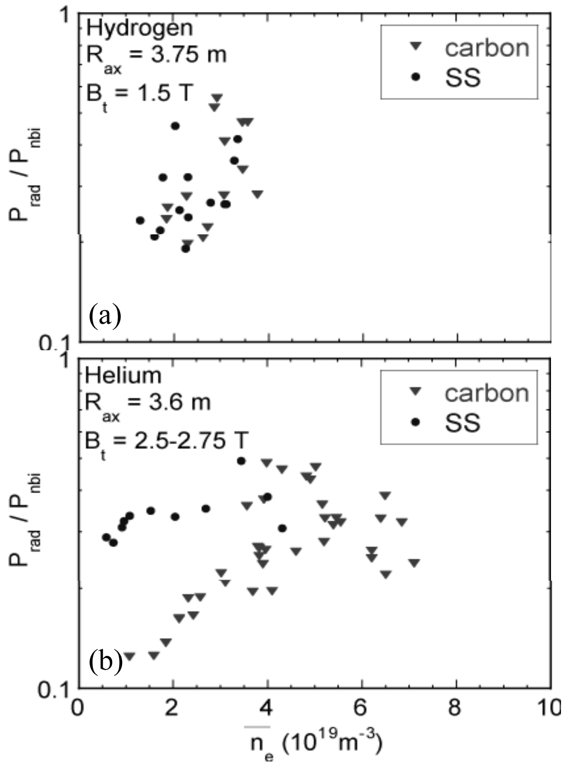

Fig. 1. Radiated power fraction versus line averaged density for (a) hydrogen gas, $R = 3.75$ m and $B_{\mathrm{axis}} = 1.5$ T and (b) helium gas, $R = 3.6$ m and $B_{\mathrm{axis}} = 2.5$–2.75 T.

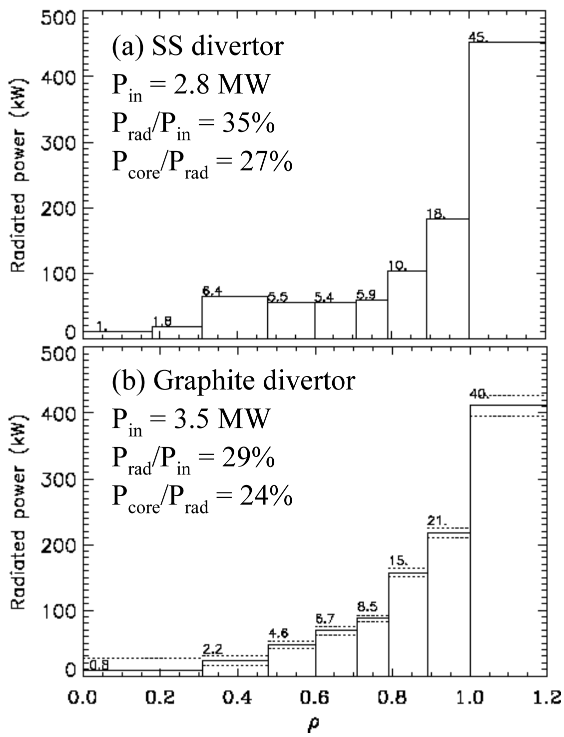

Fig. 2. Radiated power profiles for hydrogen gas, helium glow discharge cleaning, $R = 3.75$ m, $B_{\mathrm{axis}} = 1.5$ T and $n_e = 2.1 \times 10^{19}$ m^{-3} with (a) SS divertor plates (shot #3989, $t = 0.85$ s) and (b) graphite tiles (shot #8588, $t = 0.8$ s). Dashed line indicates confidence level.

measurements are made using a Schwob–Fraenkel type VUV spectrometer.

3. The effects of divertor material on short pulse radiation profiles

Between the second and third campaigns the divertor armor was changed from stainless steel (SS) plates to graphite tiles [6]. This resulted in several changes in the radiation properties. In Fig. 1, the radiated fraction versus density are compared for the cases of SS divertor plates and carbon divertor plates. In Fig. 1(b) one notes that for $R_{axis} = 3.6$ m there is a considerable decrease in the radiated power fraction at low density with graphite tiles compared to the data taken with SS plates while the data for $R_{axis} = 3.75$ m in Fig. 1(a) shows no significant difference. Looking at the radiation profile in Fig. 2(a) for $R_{axis} = 3.75$ m and hydrogen gas one notes only a small amount of core $(0 < \rho < 0.79)$ radiation with a fraction of 27% in the presence of the SS divertor plates. Compared with this SS divertor tile case, the case with graphite divertor tiles seen in Fig. 2(b) shows only a slight change in the profile shape with a negligible reduction in the core radiation fraction to 24%. The radiated fraction reduction is also negligible in agreement with the data shown in Fig. 1(a). The radiation profiles shown in Fig. 3 show basically the same picture for helium puffing with a slightly larger reduction in the core radiated fraction indicating that this result is independent of the puffed gas. Fig. 4(a) shows that with SS plates the radiated power profiles with $R_{axis} = 3.6$ m become less hollow compared to the cases with $R_{axis} = 3.75$ m shown in Figs. 2(a) and 3(a) with significant increases in the core radiation with a fraction of 44%. After the SS plates were replaced with graphite tiles the profile became much more hollow as seen in Fig. 4(b) with a reduction of the core radiation to 30% from the 44% core fraction seen in Fig. 4(a). The radiated power fraction also decreased in agreement with the data shown in Fig. 1(b). Looking at the corresponding data from a VUV spectrometer in Fig. 5 one notes that the decrease in the core radiation can be attributed to the decrease in radiation from iron, while radiation from carbon and oxygen increased. Corresponding data from soft X-ray arrays also showed a flattening of the brightness profiles with the introduction of the carbon divertor tiles.

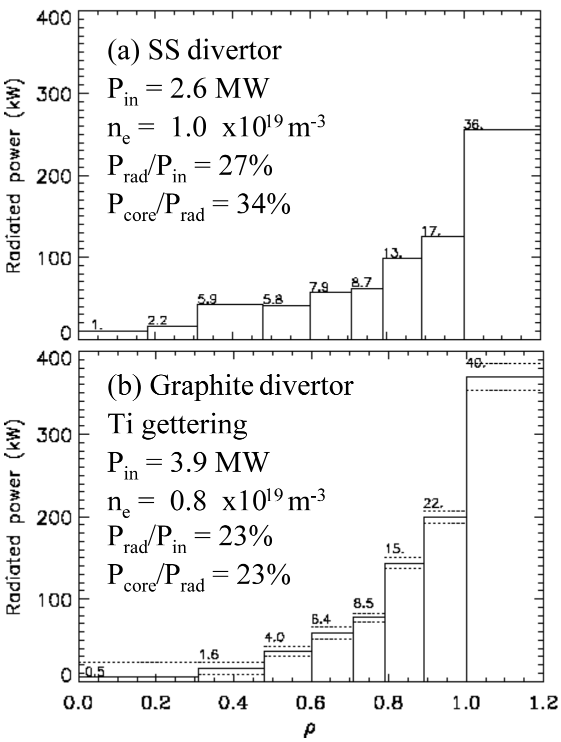

Fig. 3. Radiated power profiles for helium gas, helium glow discharge cleaning, $R = 3.75$ m and $B_{axis} = 1.5$ T with (a) SS divertor plates (shot #5834, $t = 1.3$ s) and (b) graphite tiles (shot #13938, $t = 1.72$ s). Dashed line indicates confidence level.

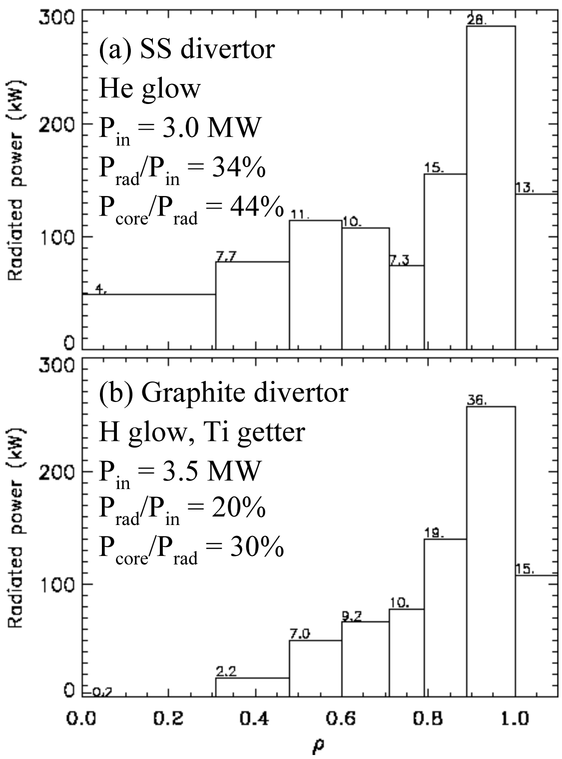

Fig. 4. Radiated power profiles for hydrogen gas, $R = 3.6$ m, $B_{axis} = 2.5–2.75$ T and $n_e = 3.3 \times 10^{19}$ m^{-3} with (a) SS divertor plates (shot #6607, $t = 1.0$ s) and (b) graphite tiles (shot #11562, $t = 1.57$ s).

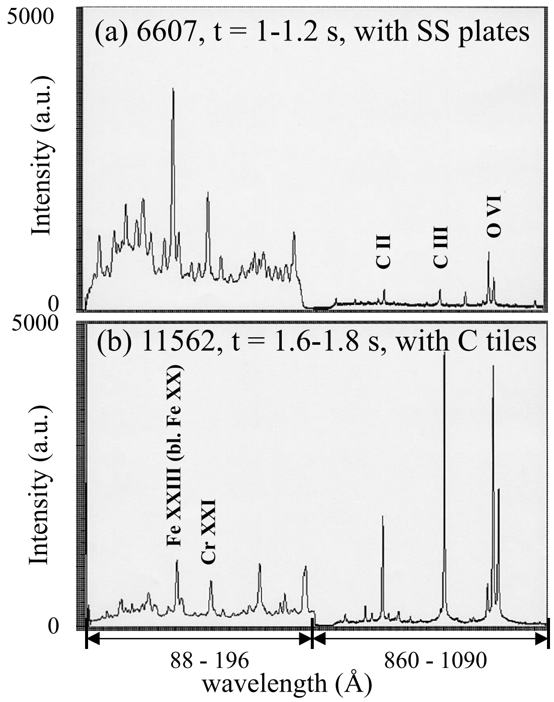

Fig. 5. Two spectra for each shot from a VUV spectrometer with (a) SS divertor plates, and (b) graphite tiles for the data corresponding to the radiation profiles shown in Fig. 4.

In addition to this evidence, that installation of the graphite divertor tiles led to the reduction of core radiation from iron, in the third campaign, we also have evidence that core radiation increased during the third campaign. In Fig. 6, radiation profiles from the middle and the end of the third experimental campaign are compared. While the radiated fractions are almost the same, there is a noticeable relative increase in the core radiation. This indicates that the amount of heavy impurities may have increased during the third campaign which was also observed in the spectroscopic measurements.

4. The effects of divertor material on long pulse radiation profiles

As has been reported elsewhere [7] a slow oscillation in the plasma parameters ($t = 1.5$ s) has been observed during long pulse experiments performed in helium with $R_{axis} = 3.75$ m during the second campaign with stainless steel divertor tiles which is known as 'breathing' plasma. Based on analysis of the radiation profile evolution from bolometer measurements it has been shown that strong oscillations in the core radiation can be attributed to oscillations in the core iron density [8]. It has been reported recently that this oscillation was limiting the density and that under similar conditions in the presence of graphite divertor tiles the oscillation did not occur and much higher densities were achieved [9]. In this paper, we extend this study by comparing the radiation profiles for discharges under similar experimental conditions with the main difference being the divertor tile material.

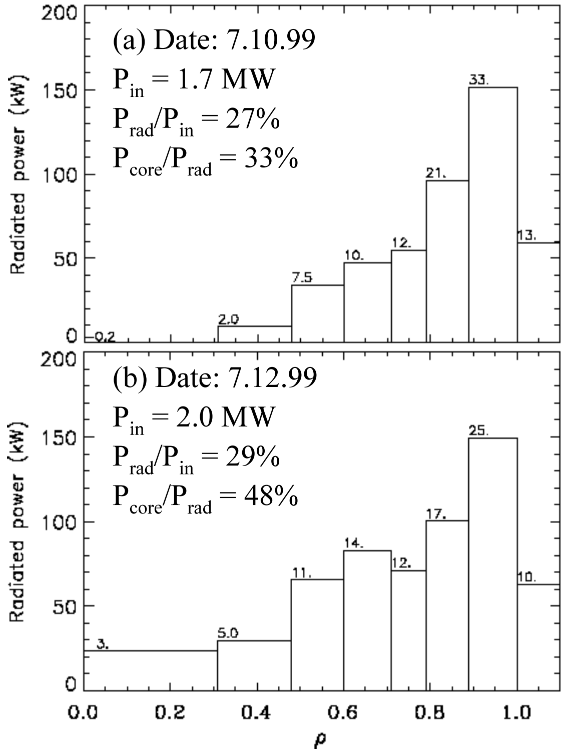

Fig. 6. Radiated power profiles for hydrogen gas, hydrogen glow discharge cleaning, titanium gettering, $R = 3.6$ m, $B_{axis} = 2.75$ T and $n_e = 2.3 \times 10^{19}$ m^{-3} from the (a) middle (shot #11551, $t = 1.37$ s) and (b) end (shot #16667, $t = 2.82$ s) of the third campaign.

Looking at the two profiles in Fig. 7 one clearly sees the difference between breathing plasma with SS divertor tiles and the quiescent plasma with graphite divertor tiles. With the SS tiles the radiated power fraction is 67% and the core radiation dominates. With graphite divertor tiles the radiation profile is hollow and the radiated power fraction is over three times lower even though the density is 40% higher.

5. Conclusions

The sputtering of the SS walls due to glow discharge cleaning may explain the slight increase in the core radiation as the campaign proceeded as was seen in Fig. 6.

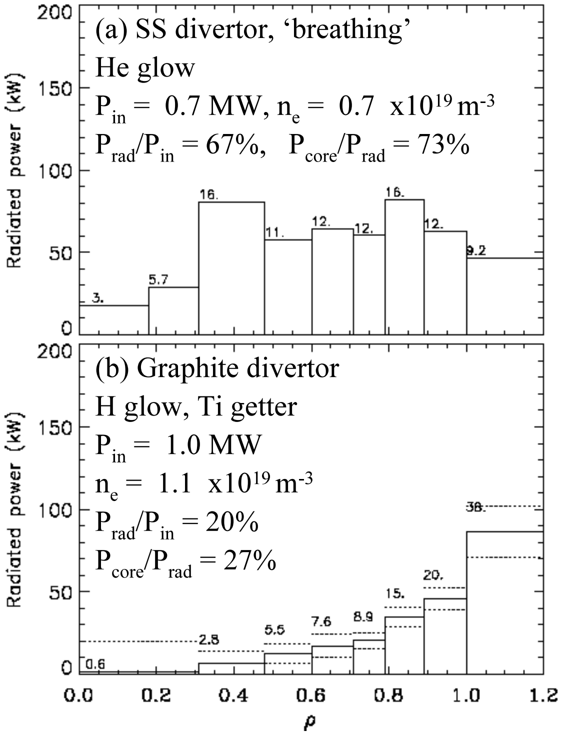

Fig. 7. Radiated power profiles for helium gas, $R = 3.75$ and $B_{axis} = 1.5$ with (a) SS divertor plates with breathing oscillation (shot #6690, $t = 5.0$ s) and (b) graphite tiles (shot #16629, $t = 2.0$ s). Dashed line indicates confidence level.

Evidence of the deposition of SS on the graphite divertor plates was seen in surface analysis measurements after the third cycle [10]. In the case of the divertor material, a large amount of data supports the conclusion that in some cases iron impurities are reduced by the substitution of graphite tiles for SS plates in the divertor. Clear evidence for this has been shown in the reduction of the radiated power fraction and the core radiation as well as the line radiation from iron seen for low density discharges at $R_{axis} = 3.6$ m. Additionally, the change in the radiation profiles under the conditions of breathing plasma after the introduction of graphite divertor tiles also supports this conclusion. However, it is still unclear as to why this effect is not seen also in the other magnetic configuration and at high density.

Acknowledgements

The authors would like to thank Director General Professor M. Fujiwara and former Director General A. Iiyoshi for their continuing support and encouragement of this research.

References

[1] R.J. Hawryluk et al., Nucl. Fus. 19 (1979) 1307.
[2] D.A. Content et al., Nucl. Fus. 30 (1990) 701.
[3] B. Lipschultz et al., Nucl. Fus. 24 (1984) 977.
[4] A. Iiyoshi et al., Nucl. Fus. 39 (1999) 1245.
[5] B.J. Peterson et al., Proceedings of the 26th EPS Conference on Controlled Fusion and Plasma Physics, Europhysics Conference Abstracts, vol. 23J, Maastricht, 1999, p. 1337.
[6] N. Noda et al., J. Plasma Fus. Res. SERIES 3 (2000) in press.
[7] Y. Takeiri et al., Plasma Phys. Control. Fusion 42 (2000) 147.
[8] B.J. Peterson et al., J. Plasma Fus. Res. SERIES 3 (2000) in press.
[9] Y. Nakamura et al., these Proceedings.
[10] S. Masuzaki, private communication.